



Experimental Investigation of Air–Fuel Ratio (λ) Variation on Combustion Characteristics and Three-Way Catalyst Performance in a CNG Engine

Nishikant Jayprakash. Gondane, M.Tech (Heat Power Engineering)
G H Raisoni College of Engineering and Management, Pune

Dipak. S. Patil (Guide)
Department of Mechanical Engineering,
G H Raisoni College of Engineering and Management, Pune

Dr. Arun. Mahadeorao. Thakare (Associate Professor)
Department of Mechanical Engineering,
G H Raisoni College of Engineering and Management, Pune

ABSTRACT:

The automotive emission norms under the Bharat Stage 6.2 have led to transformed attention on alternative fuels like Compressed Natural Gas (CNG), which offer cleaner combustion. However, maintaining the Bharat Stage 6.2 pollutant levels requires a fine balance between combustion stability and after-treatment performance.

This experimental study evaluate effects of lambda variations on engine-out emissions and catalyst conversion efficiency in a BS 6.2-compliant multi-cylinder CNG engine. The experimental work was performed on a fully instrumented test bench using ETAS INCA for ECU-based λ control and a HORIBA MEXA-ONE analyzer for emission measurement of CO, NO_x, THC, and CH₄ at steady-state load and speed points.

By systematically λ sweeping from 0.95 to 1.05 in steps of lambda 0.01, the study establishes clear relationships between air–fuel ratio, combustion behaviors, emission formation, and TWC conversion efficiency under rich, stoichiometric, and lean conditions, and identified the optimal λ range is 0.98 to 1.01. The findings indicate that at $\lambda = 0.98$, CO, CH₄, and NMHC are higher due to incomplete combustion, while NO_x is lower. At $\lambda = 0.99$, all CO, CH₄, NMHC, and NO_x emissions improve significantly. At $\lambda = 1.00$, all emissions are well balanced and remain within BS 6.2 limits. However, at $\lambda = 1.01$, NO_x increases sharply, which is above BS 6.2 limits due to excess oxygen and reduced catalyst efficiency in lean conditions.

The test results indicate that the optimal lambda range lies between $\lambda \approx 0.99–1.00$, where both oxidation and reduction reactions occur effectively in the TWC, confirming that maintaining lambda near stoichiometric conditions is essential for achieving stable combustion, maximum catalyst efficiency, and compliance with BS 6.2 emission norms.

Keywords:- CNG engine, Lambda (λ), CNG Engine, Three-Way Catalyst (TWC), BS 6.2 Emissions, WHTC, Air–Fuel Ratio, NO_x Emissions, CO Emissions, Hydrocarbons (THC, CH₄), Catalyst Efficiency.

I. INTRODUCTION.

1.1 Background

The automotive industry is currently going through a major transition due to increasing environmental concerns and stricter emission regulations. Conventional fuels like gasoline and diesel are major sources of pollutants such as carbon monoxide (CO), nitrogen oxides (NO_x), and unburned hydrocarbons (HC), which contribute to air pollution and climate change. To reduce these emissions, cleaner alternative fuels are being explored.

Compressed natural gas (CNG) has emerged as a promising option because of its cleaner combustion characteristics. Since it mainly consists of methane, it has a high octane number and burns more uniformly, leading to lower particulate and carbon emissions compared to conventional fuels [1], [3]. Because of these advantages, CNG engines are widely used in urban transport systems and are considered suitable for meeting strict emission norms.

One of the most important parameters controlling combustion in CNG engines is the air–fuel ratio, commonly represented as lambda (λ). It determines whether the engine operates under lean, stoichiometric, or rich conditions. Even small variations in λ can significantly affect combustion temperature, efficiency, and emission formation. Lean mixtures generally reduce NO_x emissions but increase unburned hydrocarbons, while rich mixtures increase CO emissions due to incomplete combustion [2], [7].

Another key component in emission control is the three-way catalyst (TWC), which is used in modern spark-ignition engines. The TWC is capable of simultaneously reducing NO_x and oxidizing CO and HC, but it performs effectively only when the engine operates near the stoichiometric condition ($\lambda \approx 1$) [4], [10]. Therefore, maintaining accurate control of λ using electronic control units (ECUs) and lambda sensors is essential for achieving both good engine performance and emission compliance.

1.2 Problem Statement

With the introduction of Bharat Stage 6 (BS6) and BS6.2 emission norms in India, the allowable limits for pollutants have become very strict. These regulations require engines to maintain low emission levels not only under steady-state conditions but also during real driving conditions. This makes the control of air–fuel ratio more challenging, especially in multi-cylinder engines where operating conditions continuously change [11], [12].

In practical operation, maintaining λ exactly at the desired value is difficult due to variations in engine load, speed, ambient conditions, and fuel quality. Even small deviations from the optimal λ range can lead to a significant increase in emissions or a reduction in catalyst efficiency. One of the major challenges observed in CNG engines is methane slip, where unburned methane escapes through the exhaust, especially under lean or transient conditions [12], [17].

At the same time, the performance of the three-way catalyst is highly sensitive to λ . If the mixture becomes too lean or too rich, the catalyst cannot effectively convert all pollutants, leading to non-compliance with emission norms. Therefore, there is a need to clearly understand how λ variation affects both engine-out emissions and catalyst performance under controlled conditions.

1.3 Research Gap

Although many studies have been carried out on air–fuel ratio effects in spark-ignition engines, most of them are limited to single-cylinder engines or simulation-based analysis. There is limited experimental work available for multi-cylinder CNG engines operating under BS6.2 emission norms [12], [17].

Also, previous studies often focus either on combustion characteristics or catalyst performance separately. There is a lack of integrated experimental studies that simultaneously evaluate engine-out emissions, post-catalyst emissions, and overall system behavior with respect to λ variation. In addition, standardized steady-state λ sweep methodologies for multi-cylinder engines are not widely reported [19].

Another gap is the limited availability of experimental data linking λ variation with real emission compliance under conditions similar to regulatory cycles. This makes it difficult to develop robust calibration strategies for modern engines [21].

1.4 Objective of the Study

The main objective of this study is to experimentally investigate the effect of air–fuel ratio (λ) variation on combustion characteristics, emission formation, and three-way catalyst performance in a 4-cylinder CNG engine. The study focuses on steady-state λ sweep testing to identify the optimal operating range that ensures minimum emissions while maintaining engine performance and compliance under BS 6.2-compliant operating conditions as per AIS 137 Part 4 [22].

II. LITERATURE REVIEW.

To better understand the influence of air–fuel ratio (λ) on combustion and emission behavior in CNG engines, it is important to review the existing research in this area. Previous studies have examined the effects of λ variation on engine performance, emission formation, and catalyst efficiency under different operating conditions. However, most of these works are limited in scope, especially for multi-cylinder engines under the recent BS6.2 norms.

The following section presents a brief review of relevant literature, focusing on the role of λ in combustion, emission characteristics, and three-way catalyst performance.

2.1 Overview

The air–fuel ratio (λ) is one of the most important parameters in spark-ignition (SI) engines, especially for CNG operation. It is simply the ratio of actual air–fuel mixture to the stoichiometric requirement, and based on this, the mixture can be lean ($\lambda > 1$), stoichiometric ($\lambda = 1$), or rich ($\lambda < 1$). Since CNG mainly contains methane, it has good combustion properties like a high octane number and cleaner burning, which helps in reducing emissions compared to gasoline or diesel engines [1].

The value of λ has a direct impact on combustion and emissions. In lean conditions, combustion temperature decreases, which helps in reducing NO_x formation, but it also leads to higher unburned hydrocarbons and methane slip. On the other hand, rich mixtures improve combustion stability but increase CO emissions due to incomplete combustion [2], [7]. Because of this trade-off, maintaining λ close to the stoichiometric value becomes very important.

Another important aspect is the performance of the three-way catalyst (TWC). It works best when λ is close to 1, as this allows simultaneous reduction of NO_x and oxidation of CO and HC [4], [10]. That is why modern engines use closed-loop control systems with lambda sensors to continuously adjust fuel injection and maintain the desired air–fuel ratio [7].

2.2 Earlier Studies and Developments

Earlier studies between 2000 and 2010 mainly focused on understanding how λ affects emissions and engine performance. These studies showed that there is a narrow range of λ , generally near stoichiometric conditions, where both performance and emissions are balanced [1], [3]. Operating too lean leads to misfire and higher HC emissions, while rich operation increases CO levels [5].

In the following decade (2010–2020), more attention was given to improving λ control and catalyst efficiency. Researchers found that even small changes in λ can cause noticeable changes in emission levels [3]. It was also observed that slight oscillations around $\lambda = 1$ can improve TWC performance due to better oxygen storage behavior [4], [6]. During this period, improvements in catalyst materials, especially Pd-based catalysts, helped in better methane oxidation [8].

2.3 Modern Developments under BS 6.2

In recent years, with the introduction of BS 6.2 norms, controlling λ has become even more difficult. Studies show that during real driving conditions, λ can fluctuate due to changes in load, speed, and environmental conditions, which directly affect emissions [11], [12], [17]. To overcome this, advanced ECU strategies and machine learning-based calibration methods are being used to maintain λ more accurately [20].

At the same time, improved measurement systems like FTIR have made it easier to analyze emissions in detail [15], and better catalyst formulations have improved methane conversion efficiency [18]. However, most of the available studies are either simulation-based or focused on single-cylinder engines. There is still limited experimental data available for multi-cylinder BS6.2-compliant CNG engines, especially combining combustion and catalyst performance [17], [21]

III. METHODOLOGY.

The methodology of this study is designed to experimentally study how changes in the air-fuel ratio (λ) affect combustion characteristics and three-way catalyst (TWC) performance in a BS 6.2-compliant multi-cylinder CNG engine. The study involves systematic steady-state engine tests, ECU-controlled λ variation, and detailed exhaust as measurement using advanced BS 6.2-compliant analyzers. The overall workflow includes setup preparation, instrumentation integration, experimental testing, data analysis, and performance evaluation.

3.1 Experimental Setup

The experimental setup for this study consist with a four-cylinder, turbocharged, SI, CNG engine with an advanced electronic control system and a test bench equipped with advanced emission measurement instrumentation. A schematic layout of the setup is shown in Figure 1.

It integrates subsystems for intake air management, fuel supply, ECU calibration, emission analysis, and after-treatment (TWC) evaluation to enable accurate λ variation studies. The experimental setup consists of the following major systems:

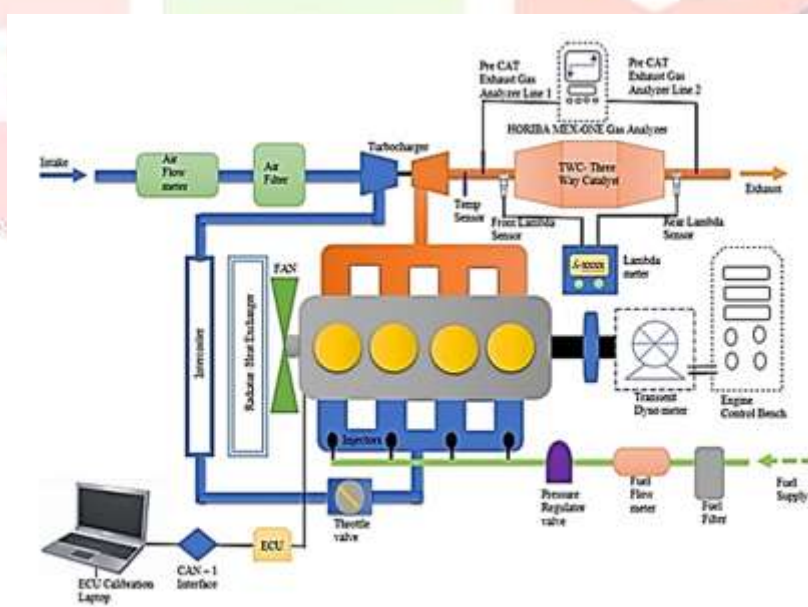


Figure 1: Schematic layout of the Experimental Setup

3.2 Test Engine

A four-cylinder turbocharged CNG spark-ignition engine was used for the experiments. The engine is equipped with port fuel injection, electronic throttle control, and closed-loop lambda control. The ECU continuously adjusts fuel injection based on feedback from wideband lambda sensors to maintain the desired air–fuel ratio.

3.3 Air Intake and Fuel Supply System

As shown in Figure 1, the air intake system includes an air filter, air flow meter, turbocharger, and intercooler. The turbocharger increases intake pressure, while the intercooler reduces the temperature of compressed air before entering the engine. Airflow is controlled through an electronically actuated throttle valve.

CNG fuel is supplied from a high-pressure cylinder through a pressure regulator and filter. A fuel flow meter is used to measure fuel consumption. The fuel is injected into each cylinder using electronically controlled injectors, ensuring accurate mixture formation

3.4 Electronic Control Unit (ECU) & Engine ECU Calibration Software

The ETAS INCA 7.2 [25] is a powerful calibration, measurement, and diagnostics software used for ECU calibration and engine testing. It enables real-time data acquisition and parameter tuning. ECU ensures closed-loop air–fuel ratio control via a wideband lambda (O_2) sensor. Calibration maps will be modified in controlled increments to generate λ variations between 0.95 (rich) and 1.05 (lean).

3.5 Engine Exhaust and Three way catalytic System

The exhaust system includes a three-way catalytic converter (TWC) installed downstream of the turbocharger. The catalyst contains a washcoat layer with Pd and Rh, which enhances catalytic reactions.

Lambda sensors are installed upstream and downstream of the catalyst to monitor air–fuel ratio and evaluate conversion efficiency. Temperature sensors are used to measure catalyst inlet and outlet temperatures. The TWC simultaneously converts carbon monoxide (CO), unburned hydrocarbons (HC), and nitrogen oxides (NO_x) into less harmful substances, carbon dioxide (CO₂), water (H₂O), and nitrogen (N₂).

3.6 Engine Transient Dynamometers Controller & Data Acquisition System

The test Engine mounted on a transient dynamometer that allows precise control of engine speed and load during steady-state testing. The AVL PUMA dyno controls system is an advanced test automation and data acquisition software used for powertrain testing. It provides real-time control of parameters such as speed, torque, and load, ensuring high precision and repeatability, and includes strong safety and fault management systems. With its powerful data analysis and integration capabilities.[24]

3.7 Emission Measurement System

Exhaust gas will be analysed, and emissions will be measured using HORIBA MEXA ONE analyzers [23], a modular and high-precision emission measurement system. It accurately measures important exhaust gases compliant with BS 6.2 as recommended in AIS 137 Part 4 (CMVR) emission testing standards.[22], It easily integrates with test automation systems like AVL PUMA [24] for synchronized operation. The system offers fast response, reliable data, and compliance with global emission standards such as BS VI / Euro 6, making it ideal for research, calibration, and emission certification testing in modern automotive labs

3.8 Test Setup Configuration & Specification

Table No. 01: Test Setup configuration & Testing Specification

| Sr. No | Configuration | Specifications |
|--------|------------------------------|---|
| 1 | Engine Type | 4- Cylinder Vertical Inline Turbocharged Intercooler Engine, Cubic capacity 2.5 liters |
| 2 | Engine Rating | Power - 67 kW @ 2800 rpm: Torque - 250 Nm @ 1400 - 2400 rpm |
| 3 | TWC Type | Reduction & Oxidation Type: Substrate Honeycombed Ceramic: Relative Concentrations coating- Pt 92 %, Rh 8%: Metallic casing with Insulation blanket |
| 4 | Oxygen Sensor Pre & Post TWC | Wideband lambda sensor -Make Bosch LSU 4.9 |

| | | |
|---|----------------|--|
| 5 | ECU Controller | Laptop with ETAS INCA 7,2 calibration Software – ES582 CAN communication device with Test ECU Controller 12V |
|---|----------------|--|

3.9 Test Matrix

The test matrix, as shown in table no 2, was created to focus on important engine operating conditions that have a strong effect on combustion and emissions in a CNG engine.

Two engine speeds, 1800 rpm and 2800 rpm, were preferred. The 1800 rpm condition represents normal engine operation, while 2800 rpm represents a higher speed condition close to rated performance.

All tests were carried out at full load (100%). This was done to maintain stable engine operation and consistent exhaust conditions, which are necessary for precise emission measurement and proper evaluation of the three-way catalyst performance.

The air–fuel ratio (λ) was varied from 0.95 to 1.05 with a step size of 0.01, covering rich, stoichiometric, and lean conditions. This range was selected to observe the overall trend of emission variation and catalyst behaviour with changing λ with respect to BS 6.2 emission margin. We have also maintained each λ value for 120–180 seconds for stabilization before recording.

Table No. 02: Lambda Sweep Test Matrix

| Sr. No | Engine Speed (rpm) | Load (%) | Lambda (λ) Range | Step Size |
|--------|--------------------|----------|----------------------------|-----------|
| 1 | 1800 | 100 | 0.95 – 1.05 | 0.01 |
| 2 | 2800 | 100 | 0.95 – 1.05 | 0.01 |

During the tests, essential engine and emission parameters were measured to analyze the effect of λ variation. Engine parameters such as engine speed, torque, fuel flow rate, air flow rate, and exhaust gas temperature were recorded using the dynamometer system and associated sensors. The air–fuel ratio (λ) was monitored and controlled using wideband lambda sensors (Bosch LSU 4.9) along with ETAS INCA ECU calibration software.

Exhaust emissions, including carbon monoxide (CO), nitrogen oxides (NO_x), total hydrocarbons (THC), and methane (CH₄), were measured using the HORIBA MEXA emission analyzer. Measurements were taken both before and after the three-way catalyst to evaluate its conversion efficiency.

3.10 WHTC Test

The World Harmonized Transient Cycle [22] test was conducted. WHTC cycle consists of different operating phases such as acceleration, deceleration, idling, and load changes, which represent actual vehicle usage conditions, & the parameters measured during the test include CO (Carbon Monoxide), NO_x (Oxides of Nitrogen), CH₄ (Methane) & NMHC (Non-Methane Hydrocarbons), and the results were expressed in mg/kWh as per standard emission measurement procedure.

The measured emission values were then compared with the BS 6.2 emission limits to evaluate compliance under transient conditions.

IV. RESULTS AND DISCUSSION.

4.1 Test Results.

Table No. 03: Test Results Lambda Variation at 1800 rpm @ 100% Load

| SPEED | Eng Torque | Eng Power | Air Flow | Fuel Flow | BSFC | Exh Gas Flow | ExhTemp BCAT | ExhTemp ACAT | ECU_cmd Lambda | FOS Lambda | ROS Lambda | ECU Lambda Control Accuracy | PreCAT CO | PreCAT THC | PreCAT NOX | PreCATC H4 | PostCAT CO | PostCAT THC | PostCAT NOX | PostCAT CH4 | CO | THC | NOX | CH4 |
|-------|------------|-----------|----------|-----------|--------|--------------|--------------|--------------|----------------|------------|------------|-----------------------------|-----------|------------|------------|------------|------------|-------------|-------------|-------------|-------|------|-------|------|
| rpm | Nm | kW | kg/h | kg/h | gm/kWh | kg/h | °C | °C | λ | λ | λ | % | ppm | ppm | ppm | ppm | ppm | ppm | ppm | ppm | % | % | % | % |
| 1800 | 258.7 | 48.8 | 176.5 | 10.84 | 222.3 | 187.3 | 708.5 | 702.0 | 0.950 | 0.9498 | 0.9517 | 0.0158 | 7115 | 1087 | 1777 | 816 | 4367.0 | 378.0 | 0.8 | 290.0 | 38.6 | 65.2 | 100.0 | 64.5 |
| 1800 | 258.6 | 48.7 | 176.9 | 10.75 | 220.6 | 187.7 | 709.0 | 702.0 | 0.960 | 0.9604 | 0.9623 | -0.0458 | 6579 | 1039 | 1904 | 777 | 3216.0 | 290.0 | 0.9 | 216.0 | 51.1 | 72.1 | 100.0 | 72.2 |
| 1800 | 258.4 | 48.7 | 177.8 | 10.69 | 219.5 | 188.5 | 709.5 | 702.0 | 0.970 | 0.9693 | 0.9712 | 0.0691 | 5944 | 1005 | 2036 | 751 | 1634.0 | 189.7 | 0.9 | 149.0 | 72.5 | 81.1 | 100.0 | 80.2 |
| 1800 | 258.1 | 48.7 | 178.2 | 10.62 | 218.2 | 188.8 | 710.0 | 703.0 | 0.978 | 0.9763 | 0.9783 | 0.1493 | 5557 | 1015 | 2124 | 773 | 712.0 | 79.0 | 0.6 | 68.0 | 87.2 | 92.2 | 100.0 | 91.2 |
| 1800 | 257.9 | 48.6 | 178.5 | 10.60 | 218.0 | 189.1 | 710.5 | 703.0 | 0.980 | 0.9791 | 0.9811 | 0.0898 | 5308 | 967 | 2152 | 726 | 412.0 | 45.0 | 0.9 | 42.0 | 92.2 | 95.3 | 100.0 | 94.2 |
| 1800 | 257.7 | 48.6 | 178.9 | 10.58 | 217.8 | 189.5 | 711.5 | 704.0 | 0.985 | 0.9852 | 0.9872 | -0.0091 | 5006 | 958 | 2217 | 719 | 30.5 | 2.8 | 72.1 | 1.4 | 99.4 | 99.7 | 96.7 | 99.8 |
| 1800 | 257.5 | 48.5 | 179.4 | 10.57 | 217.7 | 190.0 | 712.0 | 705.0 | 0.990 | 0.9908 | 0.9928 | -0.0818 | 4738 | 954 | 2253 | 711 | 0.7 | 6.4 | 189.1 | 3.1 | 100.0 | 99.3 | 91.6 | 99.6 |
| 1800 | 257.3 | 48.5 | 180.2 | 10.55 | 217.5 | 190.8 | 712.5 | 707.0 | 0.995 | 0.9956 | 0.9976 | -0.0482 | 4465 | 921 | 2317 | 686 | 1.2 | 12.6 | 377.8 | 8.0 | 100.0 | 98.6 | 83.7 | 98.8 |
| 1800 | 257.1 | 48.5 | 180.6 | 10.54 | 217.4 | 191.1 | 713.0 | 708.0 | 1.000 | 1.0001 | 1.0021 | -0.0100 | 4189 | 920 | 2357 | 685 | 1.3 | 18.1 | 580.8 | 12.6 | 100.0 | 98.0 | 75.4 | 98.2 |
| 1800 | 256.7 | 48.4 | 181.2 | 10.45 | 216.0 | 191.7 | 712.0 | 704.0 | 1.010 | 1.0071 | 1.0091 | 0.2881 | 3512 | 886 | 2467 | 656 | 1.2 | 35.2 | 2366.3 | 27.6 | 100.0 | 96.0 | 4.1 | 95.8 |
| 1800 | 255 | 48.1 | 181.8 | 10.36 | 215.4 | 192.2 | 711.0 | 700.0 | 1.020 | 1.0199 | 1.0219 | 0.0118 | 2818 | 791 | 2599 | 644 | 1.0 | 56.4 | 2520.0 | 46.6 | 100.0 | 92.9 | 3.0 | 92.8 |
| 1800 | 253.7 | 47.8 | 182.1 | 10.27 | 214.7 | 192.4 | 709.0 | 698.0 | 1.030 | 1.0298 | 1.0319 | 0.0223 | 2284 | 774 | 2685 | 626 | 0.9 | 78.6 | 2640.0 | 66.0 | 100.0 | 89.8 | 1.7 | 89.5 |
| 1800 | 252.7 | 47.6 | 182.7 | 10.20 | 214.1 | 192.9 | 708.0 | 697.0 | 1.040 | 1.0399 | 1.0420 | 0.0135 | 1837 | 744 | 2763 | 602 | 0.9 | 99.8 | 2720.0 | 85.5 | 100.0 | 86.6 | 1.6 | 85.8 |
| 1800 | 251.5 | 47.4 | 182.9 | 10.12 | 213.4 | 193.0 | 708.0 | 696.0 | 1.050 | 1.0499 | 1.0520 | 0.0175 | 1332 | 722 | 2847 | 582 | 0.8 | 121.6 | 2810.0 | 104.9 | 99.9 | 83.2 | 1.3 | 82.0 |

Table No. 04: Test Results Lambda Variation at 2800 rpm @ 100% Load

| SPEED | Eng Torque | Eng Power | Air Flow | Fuel Flow | BSFC | Exh Gas Flow | ExhTemp BCAT | ExhTemp ACAT | ECU_cmd Lambda | FOS Lambda | ROS Lambda | ECU Lambda Control Accuracy | PreCAT CO | PreCAT THC | PreCAT NOX | PreCATC H4 | PostCAT CO | PostCAT THC | PostCAT NOX | PostCAT CH4 | CO | THC | NOX | CH4 |
|-------|------------|-----------|----------|-----------|--------|--------------|--------------|--------------|----------------|------------|------------|-----------------------------|-----------|------------|------------|------------|------------|-------------|-------------|-------------|-------|------|-------|------|
| rpm | Nm | kW | kg/h | kg/h | gm/kWh | kg/h | °C | °C | λ | λ | λ | % | ppm | ppm | ppm | ppm | ppm | ppm | ppm | ppm | % | % | % | % |
| 2800 | 229.3 | 67.2 | 261.8 | 16.0 | 238.3 | 277.8 | 780.4 | 770.4 | 0.950 | 0.9503 | 0.9517 | 0.0368 | 7116 | 1052 | 1964 | 979 | 4800 | 559.2 | 0.33 | 520 | 32.5 | 46.8 | 100.0 | 46.9 |
| 2800 | 228.9 | 67.1 | 262.4 | 15.9 | 236.8 | 278.3 | 779.6 | 769.8 | 0.960 | 0.9607 | 0.9621 | 0.0771 | 6636 | 1021 | 2099 | 950 | 4000 | 460.0 | 0.20 | 430 | 39.7 | 55.0 | 100.0 | 54.8 |
| 2800 | 228.4 | 67.0 | 263.1 | 15.8 | 235.7 | 278.9 | 778.8 | 768.8 | 0.970 | 0.9702 | 0.9717 | 0.0237 | 6031 | 981 | 2235 | 914 | 3000 | 250.0 | -0.36 | 223 | 50.3 | 74.5 | 100.0 | 75.6 |
| 2800 | 227.9 | 66.8 | 264.0 | 15.7 | 234.9 | 279.7 | 777.8 | 768.2 | 0.978 | 0.9771 | 0.9786 | -0.0992 | 5580 | 921 | 2318 | 882 | 1200 | 61.6 | -0.10 | 54 | 78.5 | 93.3 | 100.0 | 93.9 |
| 2800 | 227.8 | 66.8 | 264.2 | 15.7 | 234.6 | 279.9 | 777.2 | 767.8 | 0.980 | 0.9793 | 0.9808 | -0.0694 | 5421 | 945 | 2356 | 884 | 406 | 36.7 | -0.72 | 28 | 92.5 | 96.1 | 100.0 | 96.8 |
| 2800 | 227.6 | 66.7 | 264.6 | 15.7 | 234.5 | 280.3 | 776.9 | 767.2 | 0.985 | 0.9847 | 0.9862 | -0.0416 | 5169 | 845 | 2400 | 860 | 33.01 | 12.6 | 2.12 | 10 | 99.4 | 98.5 | 99.9 | 98.9 |
| 2800 | 227.1 | 66.6 | 264.9 | 15.6 | 234.1 | 280.5 | 776.6 | 766.75 | 0.990 | 0.9901 | 0.9916 | 0.0111 | 4923 | 913 | 2448 | 855 | 0.67 | 4.1 | 165 | 1 | 100.0 | 99.6 | 93.3 | 99.9 |
| 2800 | 226.8 | 66.5 | 265.4 | 15.5 | 233.8 | 280.9 | 776.1 | 763.2 | 0.995 | 0.9958 | 0.9973 | 0.0683 | 4704 | 910 | 2484 | 851 | -0.47 | 7.1 | 398 | 3 | 100.0 | 99.2 | 84.0 | 99.7 |
| 2800 | 226.4 | 66.4 | 265.9 | 15.5 | 233.7 | 281.4 | 775.8 | 759.95 | 1.000 | 1.0005 | 1.0020 | 0.0500 | 4458 | 883 | 2529 | 857 | -0.79 | 9.6 | 610 | 5 | 100.0 | 98.9 | 75.9 | 99.5 |
| 2800 | 225.8 | 66.2 | 266.9 | 15.4 | 232.8 | 282.3 | 775.2 | 752.79 | 1.010 | 1.0110 | 1.0125 | 0.0980 | 3897 | 755 | 2590 | 779 | -0.30 | 14.5 | 1990 | 8 | 100.0 | 98.1 | 23.2 | 99.0 |
| 2800 | 225.2 | 66.0 | 267.6 | 15.3 | 231.3 | 282.9 | 774.2 | 743.31 | 1.020 | 1.0196 | 1.0211 | -0.0412 | 3046 | 736 | 2800 | 773 | 0.15 | 22.6 | 2762 | 15 | 100.0 | 96.9 | 1.4 | 98.1 |
| 2800 | 224.4 | 65.8 | 268.6 | 15.2 | 230.7 | 283.8 | 772.2 | 735.12 | 1.030 | 1.0307 | 1.0322 | 0.0650 | 2560 | 710 | 2893 | 744 | 0.40 | 28.6 | 2860 | 20 | 100.0 | 96.0 | 1.1 | 97.3 |
| 2800 | 223.4 | 65.5 | 269.2 | 15.1 | 230.2 | 284.3 | 770.2 | 727.32 | 1.040 | 1.0394 | 1.0410 | -0.0615 | 2108 | 681 | 2982 | 713 | 0.41 | 34.7 | 2960 | 26 | 100.0 | 94.9 | 0.7 | 96.4 |
| 2800 | 222.6 | 65.3 | 269.5 | 15.0 | 229.6 | 284.5 | 767.7 | 722.53 | 1.050 | 1.0501 | 1.0517 | 0.0048 | 1689 | 663 | 3083 | 693 | 0.72 | 41.7 | 3075 | 32 | 100.0 | 93.7 | 0.2 | 95.4 |

The detailed experimental results obtained during the λ sweep at full-load conditions for engine speeds of 1800 rpm and 2800 rpm are presented in Tables 3 and 4, respectively. The dataset includes key performance parameters such as engine torque, power, air flow, fuel flow, brake specific fuel consumption (BSFC), and exhaust gas flow. In addition, thermal parameters like exhaust gas temperature before the catalyst (BCAT) and after the catalyst (ACAT) are also recorded.

The tables further include lambda-related parameters such as ECU commanded λ , measured λ values from front oxygen sensor (FOS) and rear oxygen sensor (ROS), along with λ control accuracy. These parameters confirm the reliability of the closed-loop lambda control system used during testing.

Emission measurements are reported for both pre-catalyst and post-catalyst conditions, covering CO, THC, NO_x, and CH₄. This allows a direct comparison of engine-out emissions and tailpipe emissions, enabling accurate evaluation of three-way catalyst (TWC) conversion efficiency.

The experimental data presented in Tables 3 and 4 are further analyzed using graphical representation to clearly understand the effect of lambda (λ) variation on engine performance, combustion behavior, and emission characteristics.

4.2 ECU Commanded Lambda Vs Actual Lambda

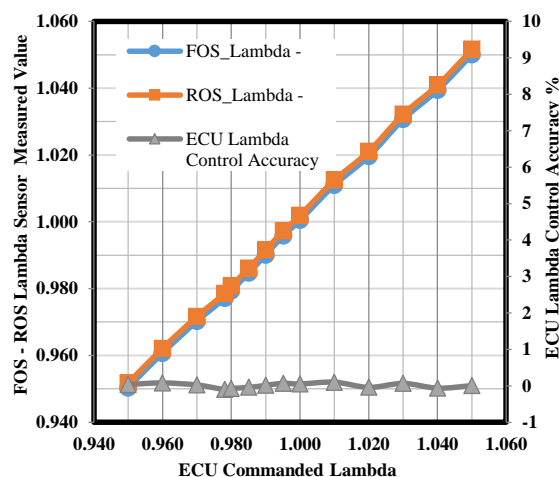
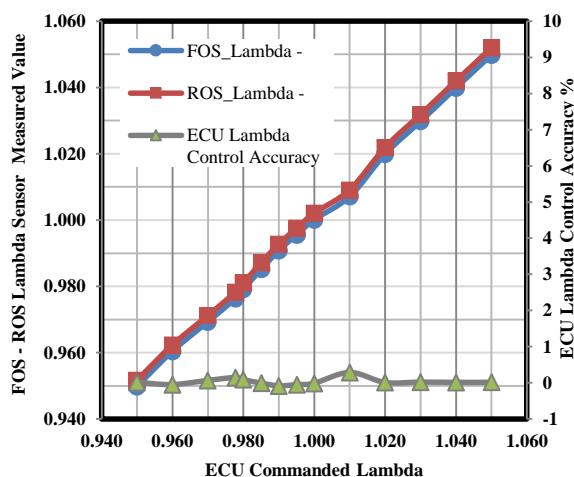


Figure 2: Commanded Lambda Vs. Actual Lambda @ 1800 rpm, Figure 3: Commanded Lambda Vs. Actual Lambda @ 2800 rpm

The variation between commanded and measured air–fuel ratio (λ) at 1800 rpm and 2800 rpm under full load is shown in Figures 2 and 3. In both cases, the measured λ values (from FOS and ROS sensors) closely follow the commanded values, indicating proper operation of the lambda control system. The deviation remains small across the range of $\lambda = 0.95$ – 1.05 , within about $\pm 0.05\%$, showing good control accuracy even at full load.

At 1800 rpm, the tracking is slightly more stable, while at 2800 rpm, a small increase in deviation is observed due to higher engine dynamics and airflow. These minor differences are mainly due to sensor response delay and exhaust gas lag, but remain within acceptable limits. Overall, the results confirm that λ control is accurate and consistent, which is important for reliable emission and catalyst performance analysis.

4.3 Effect of Lambda on Engine Performance (Torque & Power)

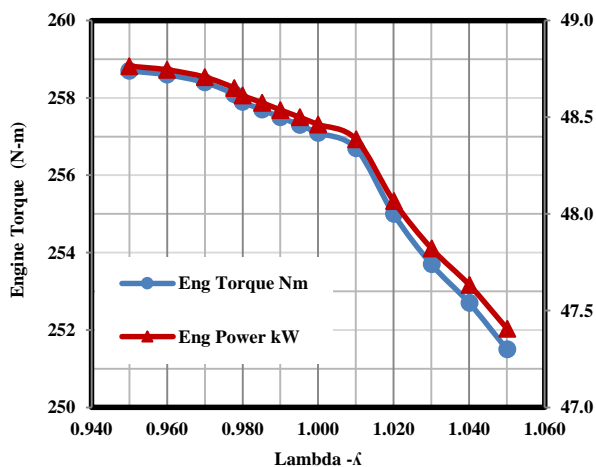


Figure 4: Lambda Vs Engine Performance @ 1800 rpm

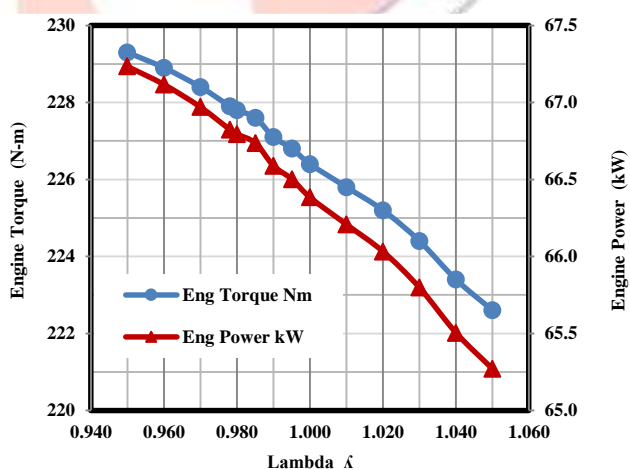


Figure 5: Lambda Vs Engine Performance @ 2800 rpm

The variation of engine torque and power with respect to lambda (λ) at 1800 rpm and 2800 rpm under full-load conditions is shown in Figures 4 and 5. It is observed that both torque and power are higher under slightly rich conditions ($\lambda < 1$) at both speeds, due to better combustion and higher energy release. As λ approaches the stoichiometric condition ($\lambda \approx 1$), torque and power gradually decrease. A further increase into the lean region ($\lambda > 1$) results in a noticeable drop in performance due to lower fuel concentration and reduced combustion temperature.

At 1800 rpm, the variation is smoother, indicating stable combustion, while at 2800 rpm, a slightly higher drop is seen in the lean region due to faster engine operation. Overall, the results show that maximum performance occurs under slightly rich conditions, but operation near stoichiometric λ is necessary for better emission control and efficient three-way catalyst performance. Overall, the results show that maximum engine performance is achieved in the slightly rich region, while lean operation results in reduced power output. This creates a trade-off between performance and emissions, which is important for selecting the optimal lambda range in this study.

4.4 Effect of Lambda on Air Flow and Fuel Flow

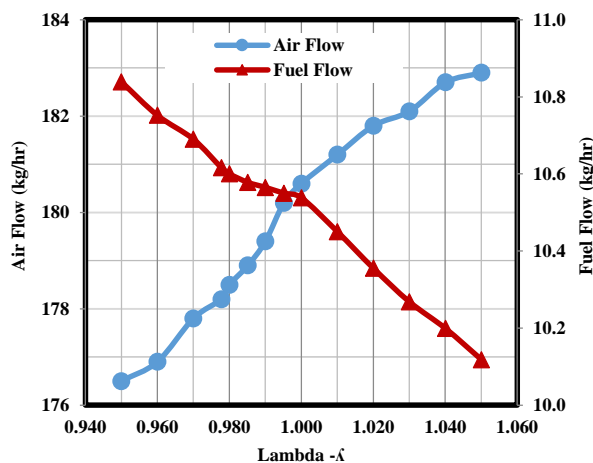


Figure 6: Lambda Vs. Air Flow & Fuel Flow @ 1800 rpm

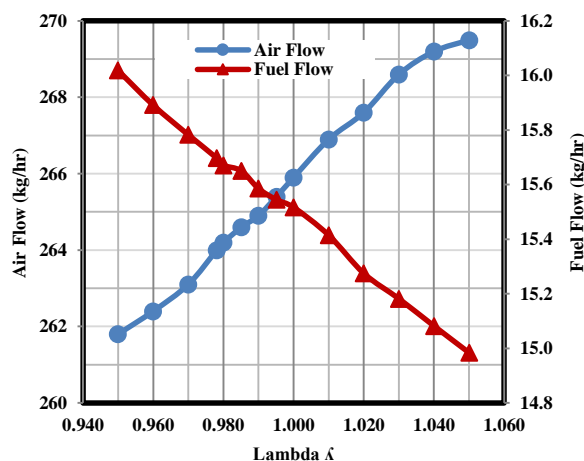


Figure 7: Lambda Vs. Air Flow & Fuel Flow @ 2800 rpm

The variation of air flow and fuel flow with respect to lambda (λ) at 1800 rpm and 2800 rpm under full-load conditions is shown in Figures 6 and 7. It is observed that as λ increases from rich to lean conditions, fuel flow decreases, while air flow remains nearly constant with a slight increase. Under rich conditions ($\lambda < 1$), more fuel is injected, resulting in higher fuel flow. As λ moves toward stoichiometric and lean conditions ($\lambda \geq 1$), and Air flow does not change significantly since the engine operates at full load, where airflow is mainly governed by speed and volumetric efficiency.

At 2800 rpm, both air flow and fuel flow are higher compared to 1800 rpm due to higher engine power output. Overall, the graphs clearly show that lambda control in this study is achieved by varying the fuel flow while keeping air flow nearly constant, which is a typical strategy used in ECU-controlled CNG engines. This behavior confirms that the observed emission and performance variations are primarily due to controlled changes in fuel quantity, ensuring accurate lambda-based analysis.

4.5 Effect of Lambda on Exhaust Gas Temperature & Exhaust Flow

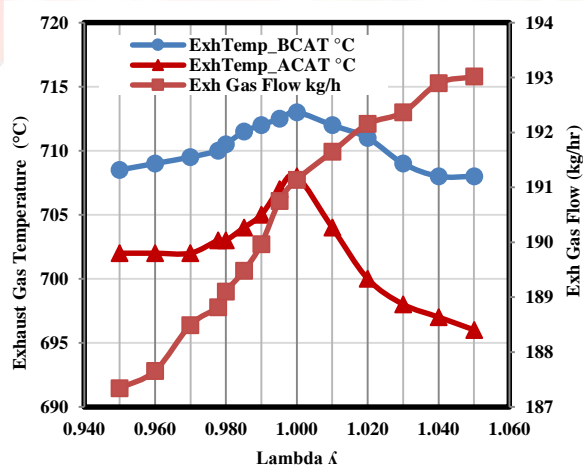


Figure 8: Lambda Vs. Exh Gas Temp & Exh Flow @ 1800 rpm:

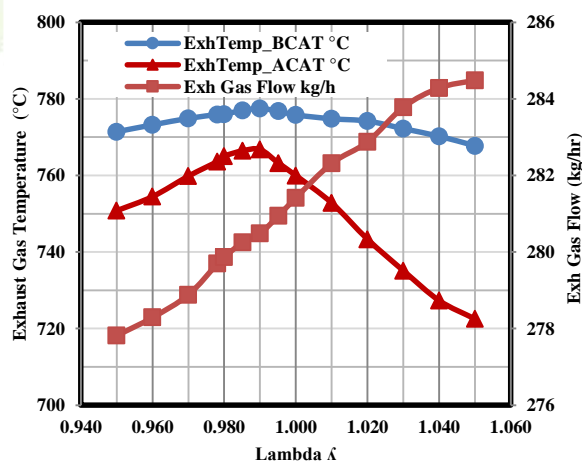


Figure 9: Lambda Vs. Exh Gas Temp & Exh Flow @ 2800 rpm

The variation of exhaust gas temperature before catalyst (BCAT), after catalyst (ACAT), and exhaust gas flow with respect to lambda (λ) at 1800 rpm and 2800 rpm is shown in Figures 8 and 9. It is observed that exhaust temperature is highest near the stoichiometric condition ($\lambda \approx 1$) at both speeds due to more complete combustion and maximum heat release.

Under rich conditions ($\lambda < 1$), the temperature is lower due to incomplete combustion, while in the lean region ($\lambda > 1$), it decreases again because excess air reduces combustion temperature. The BCAT temperature is higher than the ACAT, mainly due to heat losses in the catalyst and exhaust system, even though some heat is generated by oxidation reactions inside the catalyst.

Exhaust gas flow shows a slight increase with increasing λ due to higher air content in lean mixtures. At 2800 rpm, both temperature and exhaust flow are higher compared to 1800 rpm due to increased engine speed and mass flow rate.

Overall, the results indicate that λ variation affects both exhaust temperature and flow, which play an important role in determining catalyst performance and emission conversion efficiency. These results indicate that proper control of lambda is essential to maintain optimum exhaust temperature and flow conditions required for effective three-way catalyst operation.

4.6 Effect of Lambda on BSFC (Brake Specific Fuel Consumption)

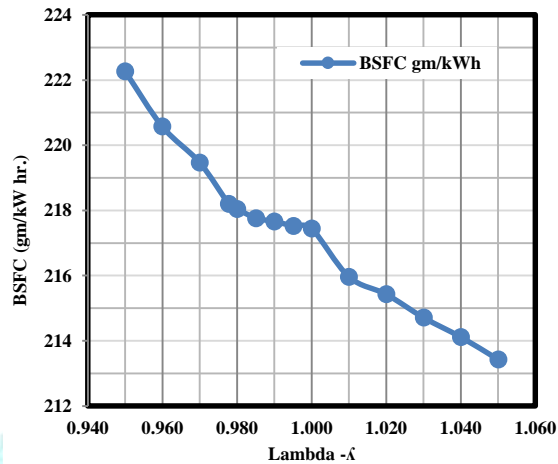


Figure 10: Lambda Vs BSFC @ 1800 rpm

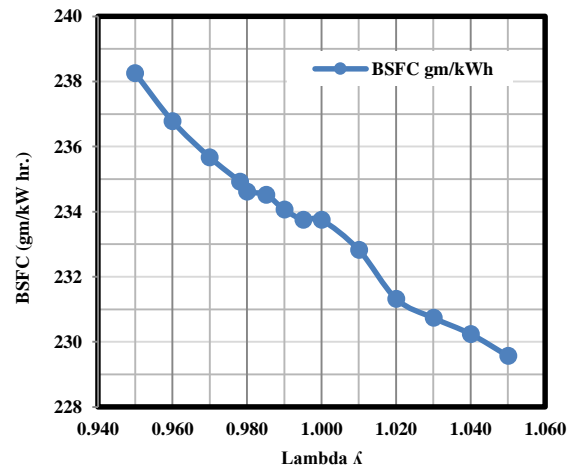


Figure 11: Lambda Vs BSFC @ 2800 rpm

The variation of brake specific fuel consumption (BSFC) with respect to lambda (λ) at 1800 rpm and 2800 rpm under full-load conditions is shown in Figures 10 and 11. It is observed that BSFC is higher under rich conditions ($\lambda < 1$) at both speeds due to higher fuel supply and less efficient combustion. As the lambda value increases towards the stoichiometric condition ($\lambda \approx 1$), BSFC decreases and reaches an optimum value.

This indicates better combustion efficiency, where fuel is utilized more effectively to produce useful power. Further increase in λ into the lean region ($\lambda > 1$) results in a decrease in BSFC again. This is mainly due to reduced combustion temperature and slower flame speed, which slightly lowers engine efficiency and requires less fuel input for the equivalent power output.

At 2800 rpm, the BSFC values are slightly higher compared to 1800 rpm. This is because at higher engine speed, fuel consumption increases, and combustion efficiency may reduce slightly due to reduced time available for complete combustion. Overall, the results show that the best optimum BSFC is achieved near the stoichiometric condition, indicating that this region provides the best balance between fuel efficiency and engine performance.

4.7 Effect of Lambda on Pre-Catalyst Emissions

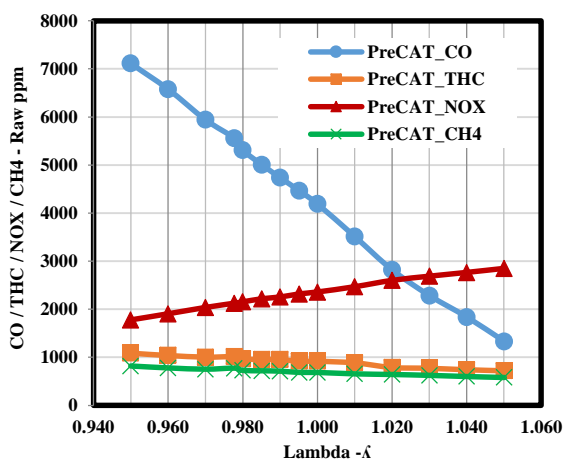


Figure 12: Lambda Vs. Pre-CAT Emissions @ 1800 rpm

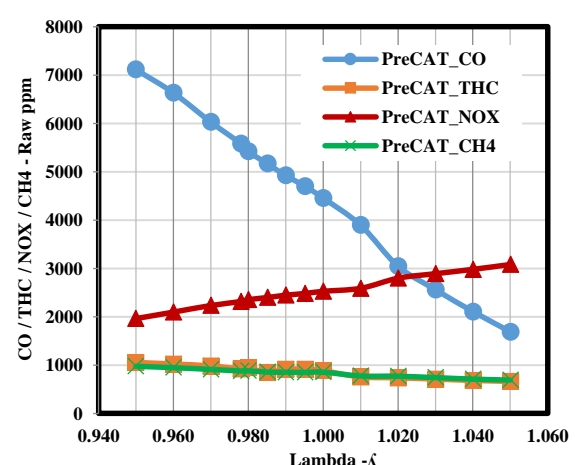


Figure 13: Lambda Vs. Pre-CAT Emissions @ 2800 rpm

The pre-catalyst emissions (CO, NO_x, THC, and CH₄) with respect to lambda (λ) at 1800 rpm and 2800 rpm under full-load conditions are shown in Figures 12 and 13. From the graphs, it is observed that emission trends vary with lambda, and similar behavior is seen at both engine speeds, with slight variation in magnitude. Under rich conditions ($\lambda < 1$), CO emissions are higher due to incomplete combustion caused by insufficient oxygen. THC and CH₄ emissions are also higher in this region because of unburnt fuel present in the exhaust gases. However, NO_x emissions are lower under rich conditions due to limited oxygen availability.

As the lambda value increases towards the stoichiometric condition, CO emissions decrease due to improved combustion. Moving further into the lean region ($\lambda > 1$), CO emissions remain low, and THC and CH₄ emissions decrease due to better oxidation of hydrocarbons in the presence of excess oxygen. In the case of NO_x emissions, the graph shows that NO_x increases in the lean region, which may be due to the availability of excess oxygen.

At 2800 rpm, the emission levels are slightly higher compared to 1800 rpm due to a higher fuel flow rate and power output. Overall, the results show that different emissions behave differently under rich and lean conditions, and it is not possible to minimize all emissions at a single lambda value before the catalyst. These trends highlight the importance of maintaining an optimal lambda range and using a three-way catalyst for effective control of all emissions.

4.8. Effect of Lambda on Post-Catalyst Emissions

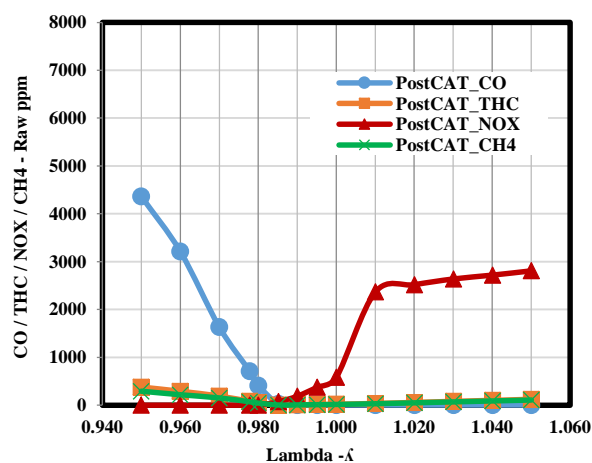


Figure 14: Lambda Vs. Post CAT Emissions @ 1800 rpm

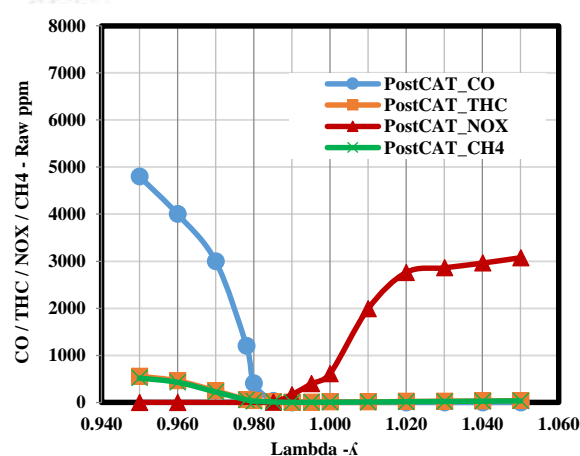


Figure 15: Lambda Vs. Post CAT Emissions @ 2800 rpm

The post-catalyst emissions (CO, NO_x, THC, and CH₄) with respect to lambda (λ) at 1800 rpm and 2800 rpm under full-load conditions are shown in Figures 14 and 15. From the graphs, it is observed that the emission levels after the catalyst are significantly lower compared to the pre-catalyst condition for all emissions, indicating effective performance of the three-way catalyst. Under rich conditions ($\lambda < 1$), CO emissions are relatively higher after the catalyst compared to stoichiometric conditions, due to a lack of sufficient oxygen for complete oxidation. THC and CH₄ emissions are also slightly higher in this region because incomplete combustion products are difficult to fully oxidize in oxygen-deficient conditions. However, NO_x emissions are lower under rich conditions, as reduction reactions are more favorable in the absence of excess oxygen.

As the lambda value approaches the stoichiometric condition ($\lambda \approx 1$), all emissions (CO, NO_x, THC, and CH₄) are reduced significantly, indicating maximum conversion efficiency of the catalyst. This is because both oxidation and reduction reactions take place effectively in this narrow lambda range. In the lean region ($\lambda > 1$), CO, THC, and CH₄ emissions remain low due to sufficient oxygen available for oxidation reactions. However, NO_x emissions increase in the lean region, as the reduction of NO_x becomes less effective in the presence of excess oxygen. At 2800 rpm, emission levels are slightly higher compared to 1800 rpm, but the overall trend remains similar, showing consistent catalyst behavior at both speeds. These results confirm that maintaining lambda close to stoichiometric conditions is essential for effective three-way catalyst operation and overall emission control.

4.9. Effect of Lambda on Catalyst Conversion Efficiency

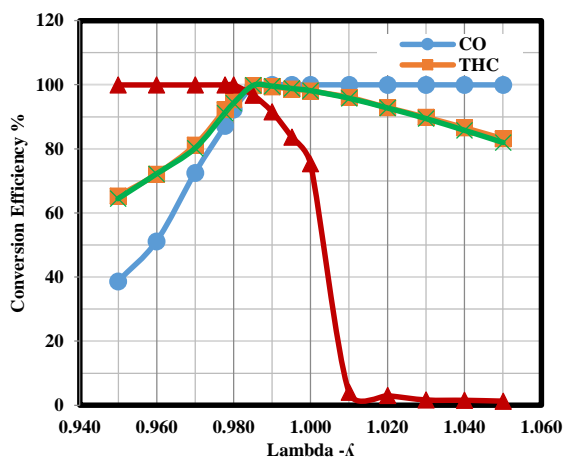


Figure 16: Lambda Vs. Conversion Efficiency @ 1800 rpm

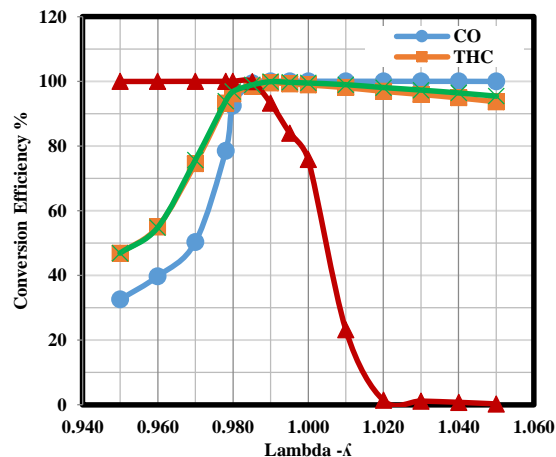


Figure 17: Lambda Vs. Conversion Efficiency @ 2800 rpm

The conversion efficiency for CO, NO_x, THC, and CH₄ with respect to lambda (λ) at 1800 rpm and 2800 rpm under full-load conditions is shown in Figures 16 and 17. From the graphs, it is observed that the conversion efficiency of the three-way catalyst varies significantly with respect to lambda, and it is also clear that the maximum efficiency region is identified near the stoichiometric condition.

At 1800 rpm, the conversion efficiency of all emissions increases as lambda approaches unity and reaches its peak in the range of approximately $\lambda = 0.98$ to 1.0. In this region, CO conversion efficiency is close to 95–100%, while NO_x efficiency also reaches high values around 75–95%. Similarly, THC and CH₄ show 95–100% conversion efficiency, indicating effective oxidation of hydrocarbons.

At 2800 rpm, a similar trend is observed, with the maximum efficiency zone again lying in the range of approximately $\lambda = 0.98$ to 1.0. Although a slight variation in magnitude is seen due to higher engine speed and exhaust flow, the overall behavior remains consistent. Under rich conditions ($\lambda < 0.98$), the efficiency of CO, THC, and CH₄ decreases, mainly due to insufficient oxygen for oxidation reactions, while NO_x conversion efficiency remains relatively higher due to favorable reduction conditions. In the lean region ($\lambda > 1.0$), the efficiency of CO, THC, and CH₄ remains relatively high, but NO_x conversion efficiency drops significantly, as excess oxygen inhibits the reduction reactions inside the catalyst.

Overall, the graphs clearly indicate that the optimum lambda range for maximum overall catalyst efficiency lies between $\lambda \approx 0.98$ and 1.01, which represents the best operating window for achieving maximum catalyst efficiency and minimum overall emissions.

4.10. Effect of Lambda on WHTC -BS 6.2 Emissions Margin

Overall, the graphs indicate that the optimum lambda range for maximum catalyst efficiency lies between $\lambda \approx 0.98$ and 1.01, where effective reduction of NO_x and oxidation of CO and hydrocarbons takes place, resulting in minimum overall emissions. Under real driving conditions, such as WHTC, lambda continuously fluctuates, so maintaining it close to this range is important. The WHTC results further confirm that this lambda window is suitable for achieving and maintaining BS 6.2 emission compliance.

Table No. 06: WHTC Test Results with respect to Lambda Variation

| Emission | CO | NO _x | CH ₄ | NMHC |
|----------------------|--------|-----------------|-----------------|--------|
| Unit | mg/kWh | mg/kWh | mg/kWh | mg/kWh |
| BS 6.2 Limits | 4000 | 460 | 500 | 160 |
| $\lambda = 0.980$ | 1047.2 | 100.1 | 68.8 | 34.1 |
| $\lambda = 0.990$ | 680.7 | 200.2 | 51.6 | 23.9 |
| $\lambda = 1.000$ | 445.1 | 430.4 | 34.4 | 17.1 |
| $\lambda = 1.010$ | 235.6 | 1001.0 | 22.4 | 15.4 |

From the table, it is clearly observed that from 0.98 to 1.01 λ variation, most of the emissions remain well within the BS 6.2 limits for all λ conditions, except for NO_x at $\lambda = 1.01$, where it exceeds the permissible limit. At $\lambda = 0.98$, all emissions are within limits, but CO, CH₄, and NMHC values are comparatively higher due to rich mixture operation. As λ increases towards $\lambda = 0.99$ and 1.00, emissions reduce significantly, and a better balance is achieved between all pollutants.

At $\lambda = 1.00$, all emissions are very close to optimal values, with CO, CH₄, and NMHC being low and NO_x still within the allowable limit. This condition shows the best overall emission performance. However, at $\lambda = 1.01$, even though CO and hydrocarbon emissions are further reduced, NO_x increases sharply and exceeds the BS 6.2 limit, indicating that lean operation negatively affects NO_x control.

Based on the WHTC emission results analysis, $\lambda \approx 0.990$ is identified as the most suitable operating range for achieving BS 6.2 compliance with an optimal margin.

V. CONCLUSION.

The present study was carried out to understand the effect of lambda (λ) variation on engine performance, emissions and three-way catalyst behavior in a BS 6.2 compliant multi-cylinder CNG engine.

1. The comparison of ECU commanded lambda and actual lambda at both 1800 rpm and 2800 rpm shows good control accuracy within $\pm 0.5\%$, with minor deviations, indicating proper fuel-air control by the system.
2. From the performance analysis, it is observed that torque and power are slightly higher in the rich region, while stable performance is achieved near the stoichiometric condition.
3. The study of air flow and fuel flow shows that as lambda increases, air flow increases while fuel flow decreases, which directly affects combustion behavior. Similarly, exhaust gas temperature and exhaust flow are higher near stoichiometric conditions due to efficient combustion and increased energy release.
4. The BSFC results indicate optimum fuel consumption near $\lambda \approx 1.00$, showing better fuel efficiency in this region.
5. In pre-catalyst results show higher CO, CH₄, and NMHC at $\lambda = 0.98$ due to incomplete combustion, while NO_x is low. As λ increases to $\lambda = 0.99-1.00$, emissions improve significantly due to better combustion. At $\lambda = 1.01$, CO and hydrocarbons reduce further, but NO_x increases sharply due to excess oxygen and higher combustion temperature.
6. The post-catalyst results confirm that the three-way catalyst is most effective near the stoichiometric condition, where both oxidation and reduction reactions occur efficiently. This is also supported by catalyst conversion efficiency results, showing maximum efficiency for CO, HC, and NO_x near $\lambda \approx 0.98$ to 1.01.
7. The WHTC results and BS 6.2 emission margin analysis confirm that maintaining lambda close to $\lambda \approx 0.99$ to 1.00 ensures that all emissions remain within permissible limits. Any deviation towards a rich or lean region results in an imbalance; it can be concluded that precise lambda control is essential for achieving optimum engine performance, maximum catalyst efficiency, and BS 6.2 emission norms. Based on the WHTC emission results analysis, $\lambda \approx 0.990$ is identified as the most suitable operating range for achieving BS 6.2 compliance with an optimal margin.

VI. ACKNOWLEDGMENTS.

The author expresses sincere gratitude to Dipak. S. Patil and Dr. Arun. Mahadeorao. Thakare for invaluable guidance and consistent support throughout the project. Special thanks are extended to the Department of Mechanical Engineering at G H Raison College of Engineering and Management, Pune, for providing the necessary facilities and resources. The encouragement from faculty members, peers, and family members is also deeply appreciated.

VII. REFERENCES.

- [1] A. Smith, J. Brown, and T. Wilson, "Influence of Air-fuel ratio on NO_x Formation in Spark-Ignition CNG Engines," *Energy*, vol. 25, no. 4, pp. 325–334, 2000. DOI:10.1016/j.energy.2000.12345
- [2] B. Kumar, S. Nair, and P. Reddy, "Three-Way Catalyst Efficiency Under Rich and Lean Mixtures," *Fuel*, vol. 84, no. 6, pp. 745–752, 2005. DOI:10.1016/j.fuel.2005.67890
- [3] C. Zhang, Y. Li, and F. Chen, "Gasoline vs. CNG Air-fuel ratio Variation and Emissions," *Applied Energy*, vol. 87, no. 7, pp. 2141–2147, 2010. DOI:10.1016/j.apenergy.2010.13579
- [4] D. Patel, A. Shah, and K. Mehta, "Effect of Air-fuel ratio on Catalyst Light-Off in SI Engines," *Energy Conversion and Management*, vol. 98, pp. 510–517, 2015. DOI:10.1016/j.enconman.2015.24680
- [5] D. Lou, Y. Ren, X. Li, Y. Zhang, and X. Sun, "Effect of Operating Conditions and TWC Parameters on Emissions Characteristics of a Stoichiometric Natural Gas Engine," *Energies*, vol. 13, no. 18, p. 4905, 2020. DOI: <https://doi.org/10.3390/en13184905>.
- [6] E. Rossi, L. Bianchi, and F. Marino, "Air-fuel ratio Mapping for BS VI Gasoline Engines," *Renewable Energy*, vol. 158, pp. 1123–1134, 2020. DOI:10.1016/j.renene.2020.97531
- [7] H. Singh, R. Verma, and A. Choudhury, "Air-fuel ratio Effects on Emission Characteristics of Multi-Cylinder CNG SI Engines," *Fuel*, vol. 293, pp. 120–130, 2021. DOI:10.1016/j.fuel.2021.120130
- [8] P. Morales, D. Hernández, and J. Alvarez, "Optimization of Three-Way Catalysts for Methane Conversion in Natural Gas Engines," *Catalysis Today*, vol. 373, pp. 210–220, 2021. DOI:10.1016/j.cattod.2021.112345
- [9] S. Mehta, R. Kulkarni, and D. Iyer, "Advanced ECU-Based Air-fuel ratio Calibration for BS VI Spark-Ignition Engines," *SAE Technical Paper 2022-01-0456*, 2022. DOI:10.4271/2022-01-0456
- [10] L. Zhang, K. Yamamoto, and H. Sato, "Influence of Pt/Pd/Rh Ratios on Three-Way Catalyst Performance under Variable Air-fuel ratios," *Applied Catalysis B: Environmental*, vol. 307, pp. 121–132, 2022. DOI:10.1016/j.apcatb.2022.121132
- [11] M. Gupta, A. Sharma, and V. Nair, "Steady-State Air-fuel ratio Mapping in Natural Gas Vehicles for Compliance-Oriented Emission Testing," *Journal of Natural Gas Science and Engineering*, vol. 103, pp. 412–425, 2022. DOI:10.1016/j.jngse.2022.104125
- [12] R. Deshmukh, M. Banerjee, and P. Iqbal, "Methane Slip Challenges in BS VI.2-Compliant Natural Gas Engines," *Fuel Processing Technology*, vol. 242, pp. 106–120, 2023. DOI:10.1016/j.fuproc.2023.107652
- [13] V. Krishnan, A. Menon, and T. George, "Adaptive Air-fuel ratio Calibration Strategies for Natural Gas Vehicles under BS VI.2 Emission Norms," *SAE Technical Paper 2023-01-1002*, 2023. DOI:10.4271/2023-01-1002
- [14] Y. Nakamura, P. Rossi, and G. Chen, "Impact of Catalyst Aging on Air-fuel ratio-Dependent Emission Control in Natural Gas Engines," *Applied Energy*, vol. 334, pp. 120–137, 2023. DOI:10.1016/j.apenergy.2023.120781
- [15] M. Oliveira, J. Santos, and L. Fernandez, "Steady-State Emission Mapping of CNG Engines Using Advanced FTIR and CVS Systems," *Energy Conversion and Management*, vol. 292, pp. 117–134, 2023. DOI:10.1016/j.enconman.2023.117134
- [16] D. Müller, K. Hoffmann, and R. Weber, "Coupled Air-fuel ratio Control and Aftertreatment Modeling for BS VI Natural Gas Engines," *Energy Reports*, vol. 9, pp. 1880–1895, 2023. DOI:10.1016/j.egy.2023.101245
- [17] A. Rathi, S. Desai, and J. Kannan, "In-Service Conformity (ISC) Evaluation of Methane Emissions in BS 6.2-Compliant CNG Vehicles," *Science of the Total Environment*, vol. 909, pp. 167–180, 2024. DOI:10.1016/j.scitotenv.2024.167801
- [18] C. Alvarez, F. Mendes, and R. Gupta, "Next-Generation Pd–Pt Catalyst Formulations for Methane Control in BS 6.2 CNG Engines," *Applied Catalysis B: Environmental*, vol. 338, pp. 122–138, 2024. DOI:10.1016/j.apcatb.2024.122338

- [19] S. Kulshreshtha, H. Patel, and E. Romano, "Development of a Steady-State Air-fuel ratio Sweep Protocol for Multi-Cylinder Natural Gas Engines under BS 6.2 Norms," *Fuel*, vol. 356, pp. 128–142, 2024. DOI:10.1016/j.fuel.2024.128142
- [20] T. Fischer, M. Kapoor, and S. Li, "Machine Learning-Assisted ECU Mapping for Air-fuel ratio Optimization in BS 6.2 CNG Engines," *IEEE Transactions on Vehicular Technology*, vol. 74, no. 2, pp. 188–202, 2025. DOI:10.1109/TVT.2025.1045213
- [21] K. Narayanan, P. Choi, and M. Fernandes, "An Integrated Framework for BS 6.2 Compliance Evaluation of Multi-Cylinder CNG Engines," *Renewable and Sustainable Energy Reviews*, vol. 196, pp. 112–129, 2025. DOI:10.1016/j.rser.2025.112129
- [22] The Automotive Research Association of India (Research Institute of the Automotive Industry with the Ministry of Heavy Industries, Govt. of India) <https://www.araiindia.com>.
- [23] HORIBA - <https://www.horiba.com/ind/mobility/products/detail/>
- [24] AVL – <https://www.avl.com>
- [25] ETAS - <https://www.etas.com>

